IOP Publishing | Royal Swedish Academy of Sciences Physica Scripta
Phys. Scr. **T161** (2014) 014007 (6pp) doi:10.1088/0031-8949/2014/T161/014007

Atomic data and collisional–radiative model for beryllium and its ions

Dmitry Kondratyev[1], Leonid Vainshtein[2], Igor Bray[3], Dmitry Fursa[3] and Yuri Ralchenko[4]

[1] Forschungszentrum Jülich GmbH, Institute of Energy and Climate Research—Plasma Physics, EURATOM Association, D-52425 Jülich, Germany
[2] P N Lebedev Physical Institute RAS, Leninsky Prospect 53, Moscow 119991, Russia
[3] ARC Centre of Excellence for Antimatter–Matter Studies, Curtin University, Perth, Western Australia, Australia
[4] National Institute of Standards and Technology, Gaithersburg, MD 20899, USA

E-mail: d.kondratyev@fz-juelich.de

Received 20 September 2013
Accepted for publication 9 December 2013
Published 2 May 2014

Abstract
In this work we present a collisional–radiative model constructed for all ionization stages of beryllium. Convergent close-coupling, *K*-matrix and Coulomb–Born-exchange methods were applied to calculate the necessary atomic data. For the neutral beryllium atom a comparison of all methods is given. Fractional ion abundances, radiative power losses and electron cooling rates were calculated as functions of electron temperature. The comparison with other available data shows a rather good agreement.

Keywords: elementary processes, beryllium, collisional–radiative model

(Some figures may appear in color only in the online journal)

1. Introduction

Beryllium is used in the ITER-like wall at JET and is foreseen as a plasma-facing material in the main chamber of ITER [1]. For interpretation of spectroscopic measurements and for modelling of the beryllium impurity behaviour in plasma, collisional atomic data (cross sections of elementary processes) are required. The 'effective' rate coefficients given in existing atomic databases (e.g. ADAS [2]) are sometimes insufficient for applications. The formation of beryllium hydrides (BeH, BeH_2) and their ions in the edge plasma, and the subsequent fragmentation directly populating excited atomic states and affecting the measured light emission can be mentioned as an example. Unfortunately due to the high toxicity of beryllium the experimental cross sections are practically unavailable in the literature. The most accurate theoretical methods, such as convergent close-coupling (CCC) [3] or the *R*-matrix with pseudostates (RMPS) [4] demand very large computation time (especially at intermediate energies when continuum coupling effects are important) and the corresponding cross sections (first of all, for transitions between excited states) are still fragmentary. To overcome the lack of data relatively simple, fast and sufficiently accurate methods such as the *K*-matrix [5] or Born (Coulomb–Born for ions) with exchange and normalization (BEN) can be applied.

In this paper, we present a collisional–radiative model (CRM) constructed for all ionization stages of beryllium. For neutral Be and selected transitions in Be^+ the sophisticated CCC method was used. The cross sections for ions Be^{2+}, Be^{3+} were computed by the ATOM code [6] using the *K*-matrix (for excitation) and the normalized Born (for ionization) methods. Also at the example of beryllium atom we present a comparison between the *K*-matrix and CCC results. Supplementary data associated with this paper (cross sections σ, rate coefficients $\langle \upsilon\sigma \rangle$ as well as the adjusted parameters for fitting formulas) are partially presented on the website [7] and are available in electronic form upon request.

In the following, we use atomic units with the Rydberg unit for energy and temperature ($\mathrm{Ry} = 13.6\,\mathrm{eV}$). Cross sections are given in the units $\pi a_0^2 = 0.8797 \times 10^{-16}\,\mathrm{cm}^2$ where a_0 is the Bohr radius. We also use the dimensionless collision strength $\Omega = g_0 \sigma E$ (here g_0 is the statistical weight of the initial state) and the designation

$$[j_1 j_2 j_3 \ldots] = (2j_1+1)^{1/2}(2j_2+1)^{1/2}(2j_3+1)^{1/2}\ldots.$$

2. Atomic data

2.1. K-matrix method

Here we confine ourselves to the consideration of transitions only between terms. The calculation of excitation cross sections based on the *K*-matrix method [5] was performed by the ATOM-AKM code [6] and consists of three parts.

(1) A chosen list of atomic states (basis) is used as an input information. Usually the basis $a = \gamma_c S_c L_c nlSL$ (where $\gamma_c S_c L_c$ describe the atomic core and nl are the principal and orbital quantum numbers of the optical electron) includes the ground state, all one-electron excitations with n from n_0 up to n_{max} and maybe a few two-electron excitations.

(2) For all pairs of states (a_i, a_f: $E_i < E_f$) from the basis, for a set of partial waves (λ_i, λ_f) of the outer electron and for total angular momenta S_T, L_T the transition amplitudes K^B (matrix elements of interaction) are calculated in *B*-approximation. Here and below we designate by the index *B* the Born (for neutral atoms) or Coulomb–Born (for ions) approximation with exchange between the incident and target electrons that we take into account using the orthogonalized wave-function method [8]. The mixing coefficients appearing in the configuration interaction expansion can be obtained from other sources (e.g. using the Cowan [9] code).

(3) From transition amplitudes the full matrix $\mathbf{K^B}$ is constructed. The final unitary scattering matrix $\mathbf{S}$ is obtained according to the matrix equation [5]

$$\mathbf{S} = \frac{\mathbf{I} + \mathrm{i}\mathbf{K^B}}{\mathbf{I} - \mathrm{i}\,\mathbf{K^B}}, \qquad (1)$$

where $\mathbf{I}$ is the diagonal identity matrix. The cross sections are expressed in terms of the $\mathbf{S}$-matrix [8]

$$\sigma(a_i - a_f) = \frac{1}{2k_i^2} \sum_{\lambda_i \lambda_f L_T S_T} \frac{[S_T L_T]^2}{[S_i L_i]^2} |S_{\Gamma_i \Gamma_f} - \delta_{\Gamma_i \Gamma_f}|^2. \qquad (2)$$

Here $\Gamma = as\lambda S_T L_T$ is a full set of quantum numbers of the total system ('atom + incident electron'), S_T and L_T are the full spin and angular momenta and k_i^2 is the energy of the incident electron before the collision.

We call such an approach the *K-matrix method*. This method allows us to correct some important shortcomings of the *B*-approximations.

(1) *Normalization.* The total flux of scattered electrons should not exceed the incident one. In any first-order method this requirement may be broken since the excitation amplitude $K^B_{\Gamma_i \Gamma_f}$ is proportional to the interaction matrix element and not limited by any condition. The $\mathbf{S}$-matrix is unitary and the requirement of electron flux conservation ('normalization') is automatically fulfilled. Normalization can considerably decrease the cross section of strong transitions, such as dipole transitions or transitions between nearby levels nl_0–nl_1. Equation (1) also includes the possibility of normalizing weak transitions on account of the strong transitions from the same initial level (normalization by another channel).

(2) *Two-step transitions.* A direct quadrupole (e.g. 2s–3d) transition cross section may be comparable (or smaller) than the two-step dipole one (2s–2p–3d). This possibility is not included in $\mathbf{K^B}$ but is provided by the transformation (1).

(3) Other less straightforward consequences of the *channel interaction* are also reflected by the *K-matrix method*.

Note that the dimensions of the matrix $\mathbf{K^B}$ grow fast with the number of included states and partial waves. The sum over λ in equation (2) converges slowly. The numerical calculations include $\lambda \leqslant \lambda_m$ (usually $\lambda_m = 28$ was used). The contribution $\Delta\sigma$ $(a_i - a_f)$ from $\lambda > \lambda_m$ is calculated in the Born approximation.

The radial functions P_{nl} of the atomic electron were obtained by numerical solution of the radial Schrödinger equation

$$\left[\frac{\mathrm{d}^2}{\mathrm{d}r^2} - \frac{l(l+1)}{r^2} + 2\frac{\zeta_c(r/\omega)}{r} + \varepsilon(nlsL)\right] P_{nl}(r) = 0 \qquad (3)$$

with the scaled $U(r) = -\frac{1}{r}\zeta_c(r/w)$ potential where the effective atomic core charge $\zeta_c(r)$ is calculated with the Slater functions. The energy parameter of the equation $\varepsilon(nlSL)$ is equal to the experimental value of the level energy (from the ionization limit) and the scale parameter ω is obtained as an equation eigenvalue. In most cases the NIST database [10] was used for $\varepsilon(nlSL)$.

2.2. Comparison of K-matrix and CCC cross sections

In order to investigate the accuracy of the *K*-matrix method we compared the collision strengths and rate coefficients for neutral Be with the results of more sophisticated CCC and RMPS calculations [11] (for RMPS only rate coefficients are published). The CCC cross sections are presented on the website [12] for transitions from the states with $n = 2$ for collision energies E up to 1000 eV. Recently Igor Bray made more accurate calculations for all transitions with $n \leqslant 4$, $E \leqslant 400$ eV. The procedure was quite similar to the one described in [3] but included more target-space states (and pseudo-states): 293 in new and 108 in old calculations [3]. For energies below 10 eV (relative to the ground state) 10 partial waves were explicitly calculated, and 16 above. Extrapolation to infinity was done using the Born approximation.

The input data for *K*-matrix calculations included the following states:

$$2s^2\ {}^1S,\ 2snl\ {}^1L,\ {}^3L,\ L = l,\ n = 2-5,\ \text{all}\ l,$$
$$2p^2\ {}^1S,\ {}^3P,\ {}^1D,\ 2p3l,\ l = 0-2$$

and the matrix CV of configuration interaction vectors. The states 2p3*l* were used only for configuration mixing. The real transitions to these states were not considered. Corresponding levels are above the ionization threshold and their contribution to the channel interaction is negligible. The total number of transitions (including the elastic scattering channels) was equal to 393. The mixing coefficients of the matrix CV were adjusted to obtain the best coincidence of the oscillator strengths *f* with the results of multiconfiguration Hartree-Fock calculations [13]. The mixing of up to four configurations was included for every group of states with the same *SL* and parity.

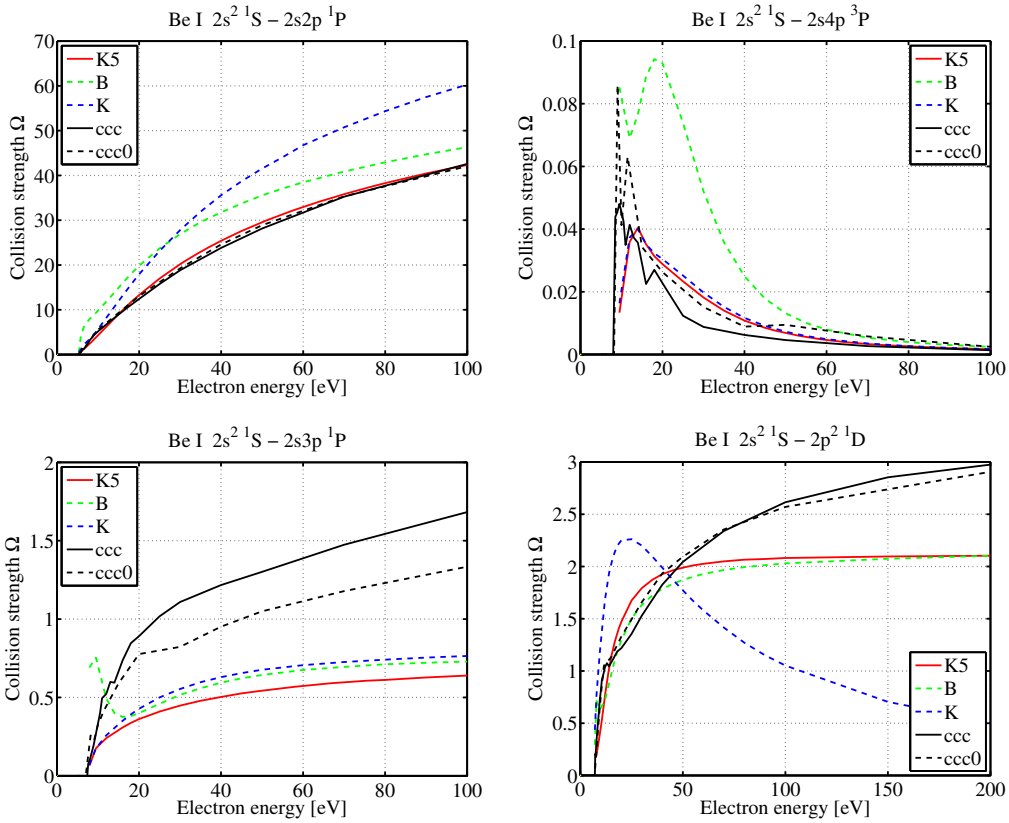

Figure 1. Collision strength Ω as a function of incident electron energy. 'K5' and 'K'—the *K*-matrix method with levels up to $n = 5$ with and without configuration interaction, 'B'—Born approximation with account of exchange, 'CCC'—convergent close-coupling method (293 states) and 'CCC0'—convergent close-coupling method [3] (106 states).

For discussion of the results it is important to distinguish two energy ranges. At large energies the collisional part of the problem is trivial: the cross section $\sigma = \sigma_B$ where σ_B is the Born cross section (without exchange if $\Delta S = 0$). The difference between the *K*-matrix and CCC data is connected with the difference of the atomic wave functions, i.e. with the configuration mixing. At small and medium energies of the scattered electron the difference in the approach to the collisional part of the problem (i.e. the normalization and the channel interaction) is important. From the present results as well as our previous calculations we can conclude that the *K*-matrix method tends to overestimate the effect of the channel interaction. We divide (perhaps rather arbitrarily) the cross sections into three groups according to the degree of agreement with CCC.

(1) *Good* agreement was obtained, as illustrated in figure 1(a), for dipole transitions, if the oscillator strength is not very small. We note also the significant influence of the configuration mixing. For intercombination transitions (figure 1(b)) the difference is somewhat larger because the exchange is normally more sensitive to the used approximations. The too-fast decrease of the CCC cross section can be connected with an insufficient number of partial waves to ensure convergence and the large peaks near the threshold (resonances due to the virtual formation of the Be-ion)—with overestimation of exchange due to the non-orthogonality of total wave functions ('residual Born–Oppenheimer').

(2) *Poor* agreement was found in cases of very strong configuration interaction when the description of the atomic structure used in ATOM can be inadequate and for transitions with extremely small values of oscillator strengths for which the cancellation effects are important (figure 1(c)).

(3) Some *problematic* cases for which we cannot give a definite explanation. One example is shown in figure 1(d). For this transition ($2s^2\,{}^1S \to 2p^2\,{}^1D$) two mechanisms are possible: the 'step' $2s^2\,{}^1S \to 2s2p^1P \to 2p^2\,{}^1D$ (with asymptotic $\Omega \sim 1/E$) and the quadrupole transition ($2s^2\,{}^1S \to 2p^2\,{}^1D$) due to configuration interaction $2s^2\,{}^1S + 2p^2\,{}^1S$ (the asymptotic for transitions with $\Delta L = 2$ is $\Omega \to$ const). The collision strength of CCC, opposite to what we expect, increases. The reason for this difference is unclear. It may be that the collision strength approaches a constant at higher energies.

In most cases the agreement between rate coefficients is usually much better than for cross sections (even when there are substantial discrepancies for them). And of course the *K*-matrix results demonstrate an essential improvement compared to the Born data.

2.3. Electron impact ionization cross sections

For the ionization of an electron from the state $a_i = \gamma_c S_c L_c n l_i S_i L_i$ of the atom (ion) X_z

$$X_z(a_i) + e(E\lambda_i) \to X_{z+1}(\gamma_c S_c L_c) + e(E_f l_f) + e(E'\lambda_f), \qquad E = E' + E_f + \Delta E \tag{4}$$

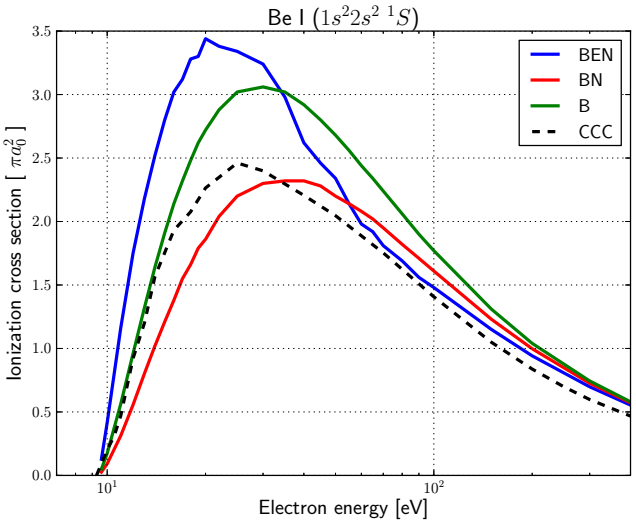

Figure 2. Electron impact ionization cross section for the Be ground state: Born (B), Born with normalization (BN), BEN and CCC calculations.

(here $\Delta E = E_z$ is the ionization threshold) the ionization cross section in the **B**-approximation is equal:

$$\sigma_{\mathrm{i}z}(nl_{\mathrm{i}}) = \sum_{l_{\mathrm{f}}S_{\mathrm{f}}L_{\mathrm{f}}} \int_0^{E_m/2} 2\sigma(a_{\mathrm{i}}, a_{\mathrm{f}})\,\mathrm{d}E_{\mathrm{f}}, \tag{5}$$

where $E_m = E - \Delta E$ and $a_{\mathrm{f}} = \gamma_{\mathrm{c}} S_{\mathrm{c}} L_{\mathrm{c}} E_{\mathrm{f}} l_{\mathrm{f}} S_{\mathrm{f}} L_{\mathrm{f}}$. In this case the final state of the atom belongs to the continuum, and therefore the continuum radial function $P_{\mathrm{f}}(r)$ must be used.

Due to the additional sum over the momenta l_{f}, S_{f}, L_{f} and the integral over the energy E_{f} of the ejected electron, the inclusion of the ionization channel in the *K*-matrix scheme becomes unreasonable (and practically impossible, which is why we did not include the ionization channels in the *K*-matrix for excitation). At the same time, due to these summations, the ionization cross section $\sigma_{\mathrm{i}z}$ is not sensitive to the channel's interaction. However the normalization effects must be included in the calculation of $\sigma_{\mathrm{i}z}$.

The ATOM code [6] calculates ionization cross sections in the *B*-approximation with additional normalization for its own (ionization channel) and some strong excitation channels (usually these are transitions to nearby levels which are dipole connected with the initial state). The method of normalization is also based on the *K*-matrix, but with some simplifications appropriate for normalization purposes, namely, the approximate (reduced) *K*-matrix contained only those matrix elements which include the initial state Γ_{i}. It means that the normalization of each $L_{\mathrm{T}}S_{\mathrm{T}}$ channel is performed independently.

The ion X_{z+1} can be produced either by direct ionization (DI) or through inner shell excitation of X_z followed by autoionization (EA). In our calculations both DI and EA processes were included. As a rule, DI dominates the total impact ionization cross section but the contribution of EA increases at energies above the corresponding threshold.

A comparison of the ionization cross section from the ground state of Be I obtained by *B* and CCC methods is shown in figure 2. The account for exchange by the orthogonalized function method [8] sometimes leads to the appearance of a noticeable (non-physical) peak in the cross section at near-threshold energies. For this reason we usually use *B*-data calculated with normalization but without exchange.

3. Collisional–radiative model

CRM constructed for all charge stages of beryllium contains 80 *LS*-terms:

Be I : $2s^2\ ^1S$; $2snl\ ^1L, ^3L$, $L = l$, $n = 2-4$, all l; $2p^2\ ^1D, ^3P$ (19 terms),
Be II : $1s^2 nl\ ^2L$, $L = l, n = 2-6$, all l (20 terms),
Be III : $1s^2\ ^1S$; $1snl\ ^1L, ^3L$, $L = l$, $n = 2-4$, all l (19 terms),
Be IV : $nl\ ^2L$, $L = l$, $n = 1-6$, all l (21 terms),
Be V (bare nucleus) : (1 state),

and includes the following processes: spontaneous radiative decays, electron impact excitation and ionization, as well as radiative, dielectronic and three-body recombination. The plasma is supposed to be optically thin. The energies of the levels and (if available) the oscillator strengths were taken from the NIST database. A new improved set of CCC excitation and ionization cross sections for neutral beryllium as well as CCC data [14] for Be^+ were used. For selected transitions in Be, Be^+ and for ions Be^{2+}, Be^{3+} the cross sections were computed by the ATOM code [6] (the *K*-matrix for excitation and the normalized Coulomb–Born-exchange for ionization). Note that the method used in ATOM corresponds to perturbation theory with a small parameter $1/Z$, where Z is the spectroscopic symbol. Therefore, the method's accuracy is expected to be better for ions. The partial photorecombination rate coefficients for all ion stages were also calculated by the ATOM code. Three-body recombination rates were obtained from the principle of detailed balance. For dielectronic recombination (DR) rates the formula suggested in [15] was used. We also assumed that DR occurs from the ground state of the target ion into the highest state of the recombined ion. This assumption is reasonable for Be with rather small resonance transition energy.

The steady-state solution of the system of balance equations for ionization equilibrium and level populations was obtained using the collisional–radiative code NOMAD [16]. As an illustration, figure 3 shows the ionization balance and radiative power loss coefficient $L_z = P_{\mathrm{rad}}/N_{\mathrm{e}}N_a$ as a function of the electron temperature, for an assumed electron density $N_{\mathrm{e}} = 10^{13}\,\mathrm{cm}^{-3}$. Here $N_a = \Sigma\ N^Z$ is the total beryllium density, P_{rad} is the radiated power ($\mathrm{W\,cm}^{-3}$) including line (due to the cascade transitions), recombination (radiative and dielectronic) and bremsstrahlung radiation

$$P_l = \sum_{Zij} 1.6\times10^{-19} N_i^Z A_{ij}^Z \Delta E_{ij}^Z, \tag{6}$$

$$P_{\mathrm{rec}} = \sum_{Zij} 1.6\times10^{-19}\left(\alpha_{ji}^{rr}\left(I_{ij}^Z + \frac{3}{2}T_{\mathrm{e}}\right) + \alpha_{ji}^{dr}\Delta\bar{E}_j^{Z+1}\right) \times N_{\mathrm{e}} N_j^{Z+1}, \tag{7}$$

$$P_{\mathrm{br}} = 1.54\times10^{-32}\bar{g}N_{\mathrm{e}}\sqrt{T_{\mathrm{e}}}\sum_Z N^Z Z^2. \tag{8}$$

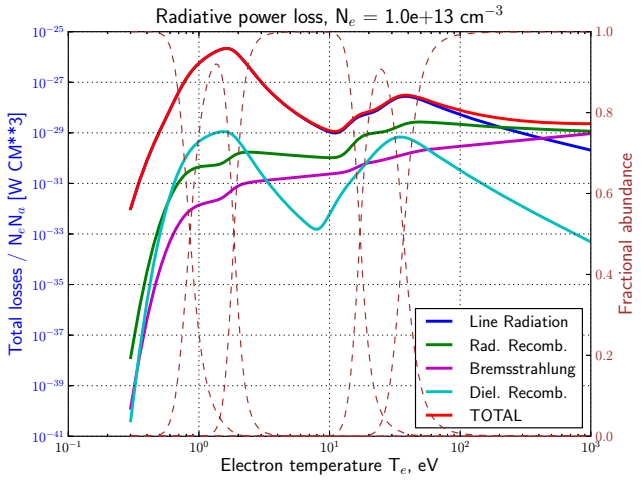

Figure 3. Radiative power loss per unit volume due to line emission, recombination radiation and bremsstrahlung as a function of electron temperature. The total power loss coefficient is shown in red. Dashed lines represent the relative concentrations of Be ions.

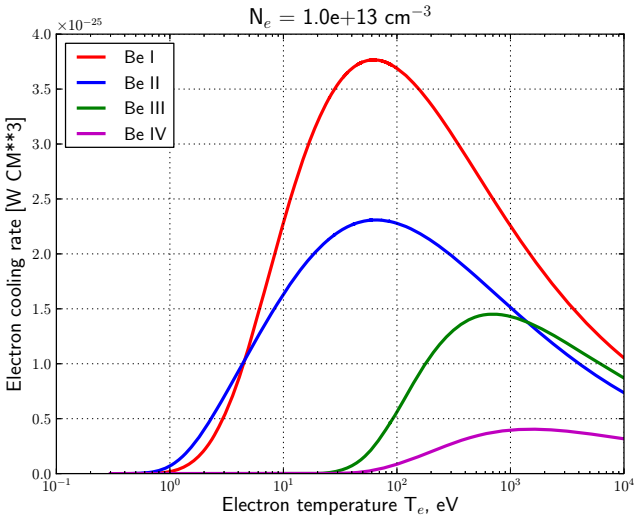

Figure 4. Electron cooling rate for different ionization stages of Be as a function of electron temperature.

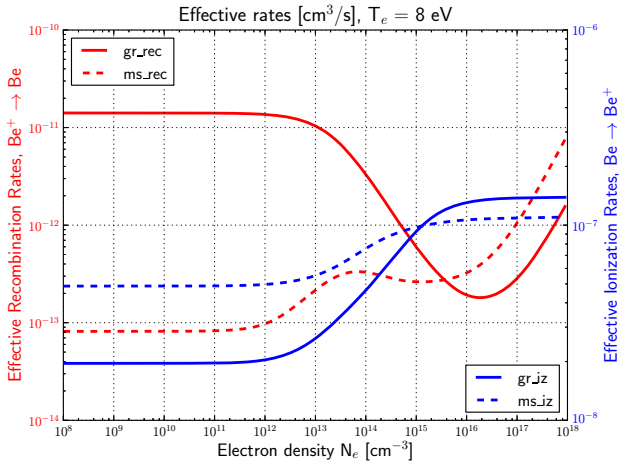

Figure 5. Effective ionization and recombination rates as a function of electron temperature for the ground ($2s^2\ ^1S$) and metastable ($2s2p\ ^3P$) states of Be I.

The summation in (6) and (7) is made over all the transitions and all ions Z. In formula (8), the frequency-averaged free–free Gaunt factor g has been taken as equal to 1.2, and T_e is expressed in eV.

The two peaks in L_z—one at low and another one at high temperatures—correspond to Be/Be$^+$ and Be^{2+}/Be^{3+} (i.e. L- and K-shell) radiation, respectively. The minimum at ≈10 eV occurs due to the fact that the most abundant He-like ions Be^{2+} cannot be excited at that temperature. Below 100 eV, L_z is dominated by bound–bound transitions. At higher temperatures beryllium becomes completely ionized and no longer produces the line radiation. The increase of density leads to a shift of the ionization equilibrium and, more importantly, to the competition of collisional deexcitation with radiative decays. As a result, the total power-loss coefficient at a given temperature decreases.

In an ionizing regime, which is of special interest for the modelling of light impurity transport, the electron cooling rate $\Lambda = P_e/N_eN_a$ (where P_e is the electron cooling power in W cm^{-3}) is dominated by excitation and ionization

$$P_{ex} = \sum_{Zij} 1.6 \times 10^{-19} N_e(\langle \upsilon\sigma_{ij}\rangle_{ex} N_i^Z - \langle \upsilon\sigma_{ji}\rangle_{dex} N_j^Z)\Delta E_{ij}^Z, \tag{9}$$

$$P_{iz} = \sum_{Zij} 1.6 \times 10^{-19} N_e(\langle \upsilon\sigma_{ij}\rangle_{iz} N_i^Z - N_e \alpha_{ji}^{3bR} N_j^{Z+1}) \times \left(I_{ij}^Z + \frac{3}{2}T_e\right). \tag{10}$$

Figure 4 demonstrates $\Lambda(T_e)$ calculated for Be ions. The comparison with other available data (the ADAS database) shows a rather good agreement.

We also performed calculations of effective ionization and recombination rates and studied their dependence on plasma parameters. The obtained coefficients will be implemented in the three-dimensional Monte-Carlo neutral transport code EIRENE [17]. The rates were derived from the total rate matrix under quasi-steady-state assumption: $dN_i/dt = 0$ for all excited states except for ground and metastable levels. An example for Be I is shown in figure 5. The essential contribution of the excited states to the effective rates is clearly seen: the effective ionization rate increases monotonically and becomes saturated at high N_e. The recombination rate behaves non-monotonically due to competition between the recombination to and the collisional ionization from excited states.

4. Conclusion

In this work, a comparison between two independent methods (*K*-matrix/Coulomb–Born-exchange and the sophisticated convergent close-coupling) is made for Be I and demonstrates reasonable agreement. Although the CCC method generally provides an excellent accuracy, the use of the *K*-matrix/BEN greatly reduces the computational efforts. Similar *K*-matrix/BEN calculations (possibly including transitions between fine structure components) can easily be done for other light (or more precisely, small-electron)

elements (e.g. for alkali or alkaline earth atoms and their isoelectronic ions).

The CRM constructed for Be ions includes a new, improved set of CCC excitation and ionization cross sections. The steady-state ionization balance, electron cooling rates and radiative power losses were calculated as functions of electron temperature by the NOMAD code. The influence of the excited states on effective ionization and recombination rate coefficients is demonstrated.

Acknowledgment

This work was supported in part (DK) by an EFDA fusion researcher fellowship. The authors would like to thank Professor Dr D Reiter and Dr O Marchuk for stimulating discussions and support of this work.

References

[1] Bolt H *et al* 2002 *J. Nucl. Mater.* **307–311** 43
[2] Summers H P 2004 *The ADAS User Manual* version 2.6 (www.adas.ac.uk)
[3] Fursa D V and Bray I 1997 *J. Phys. B: At. Mol. Opt. Phys.* **30** 5895
[4] Ballance C P *et al* 2003 *Phys. Rev.* A **68** 062705
[5] Seaton M J 1961 *Proc. Phys. Soc.* **77** 174
[6] Shevelko V P and Vainshtein L A 1993 *Atomic Physics for Hot Plasmas* (Bristol: IOP)
[7] Kondratyev D A and Vainshtein L A 2012 www-amdis.iaea.org/Atom_AKM/
[8] Sobelman I I, Vainshtein L A and Yukov E A 1995 *Excitation of Atoms and Broadening of Spectral Lines* (New York: Springer)
[9] Cowan R D 1981 *The Theory of Atomic Structure and Spectra* (Berkeley, CA: University of California Press)
[10] Kramida A *et al* 2012 *NIST Atomic Spectra Database* version 5.0 (http://physics.nist.gov/asd/)
[11] Loch S D *et al* 2008 *At. Data Nucl. Data Tables* **94** 257
[12] Bray I and Ralchenko Y 1997 http://atom.curtin.edu.au/CCC-WWW/index.html
[13] Tachiev G and Froese Fischer C 1999 *J. Phys. B: At. Mol. Opt. Phys.* **32** 5805
[14] Starobinets A *et al* 2003 *Phys. Scr.* **67** 500
[15] Mazzotta P *et al* 1998 *Astron. Astrophys. Suppl. Ser.* **133** 403
[16] Ralchenko Yu V and Maron Y 2001 *J. Quant. Spectrosc. Radiat. Transfer* **71** 609
[17] Reiter D, Baelmans M and Börner P 2005 *Fusion Sci. Technol.* **47** 172